The density of states of disordered coupled chains in a magnetic field



1989 J. Phys.: Condens. Matter 1 8841

(http://iopscience.iop.org/0953-8984/1/45/009)

J. Phys.: Condens. Matter 1 (1989) 8841–8850. Printed in the UK

# The density of states of disordered coupled chains in a magnetic field

Xiao-Dun Jing† and Zhao-Qing Zhang†‡

† Institute of Physics, Chinese Academy of Sciences, Beijing, People's Republic of China

‡ CCAST (World Laboratory), PO Box 8730, Beijing, People's Republic of China

Received 10 January 1989, in final form 11 April 1989

**Abstract.** The density of states for a tight-binding electron in disordered coupled chains with a weak Gaussian diagonal randomness is simulated using Dean's method under various magnetic fields. These data are compared with the results of the coherent-potential approximation (CPA) based on the analytic Green function obtained recently by the present authors. The CPA is shown to give quantitatively good results except in the near-tail regions. The scaling behaviour near the band edges (including the near-tail regions) are also examined in detail. It is found that, when the magnetic field is above a critical field, scaling exists and follows the one-dimensional universal function. Below this critical field, a non-universal energy shift is required before scaling can apply. The existence of this energy shift also limits the range of scaling to a smaller randomness.

## 1. Introduction

In the past few years, much attention has been focused on the universal scaling behaviour of the electronic density of states (DOS) near the band edge of weakly disordered systems. In their classic work, Halperin and Lax (HL) (1966) have presented a variational approach to the calculation of the band tail DOS. In one dimension the predictions of the HL theory have been corroborated by more exact treatments for both continuous (Halperin 1965) and discretised (Derrida and Gardner 1984) Schrödinger equations. The scaling behaviour found in the near-tail region has been extended to regions near the band edges by reducing the problem to a white-noise model (WNM) (Cohen *et al* 1985). In dimensions $2 \leqslant d < 4$, a non-universal energy shift is required before scaling can apply. For a tight-binding model with Gaussian diagonal randomness, the scaling behaviour near the band edges has been discussed in detail using the effective-medium approach (Economou *et al* 1985). According to Economou *et al* (1985), three regions can be defined qualitatively near the band edge. The first region (region I) is the region near the edge of the band coherent-potential approximation (CPA). In this region, scaling exists and the corresponding scaling relations can be obtained from the band CPA equation. The second region (region II) is the near-tail region where the scaling theory of HL applies with the same scaling relations found in region I. Since, in this region, the localisation length of the localised states is much greater than the lattice constant, the single-site CPA always underestimates the DOS. The above two regions can be joined smoothly to form a single scaling region near the band edge. The entire scaling region has been seen numerically

0953-8984/89/458841 + 10 $02.50  

in one, two and three dimensions (Zhang and Sheng 1986). The third region is the deep tail region where the localisation length of the localised states is of the order of the lattice constant. This region is non-universal and the CPA becomes valid. In one dimension the above scaling behaviour near the band edge has also been extended to the case of off-diagonal randomness (Evangelou 1987).

Recently, the present authors have formulated the Green functions (GFs) for a Bloch electron on coupled chains in a magnetic field $\gamma$ (in the units of the flux quantum) (Zhang and Jing 1989). The magnetic field is shown to open a gap in the continuous spectrum and generates various behaviours of the DOS. However, except at some special magnetic fields, all the singularities are found to be one dimensional. The analytic GFs obtained have been used to study the properties of the localised condensation of an impure ladder superconducting network (Jing and Zhang 1989).

The main purpose of this work is to study the scaling behaviour in regions I and II near the band edges of weakly disordered coupled chains in a magnetic field. In such a system, although the singularities at the band edges of the pure system are one dimensional, it is not clear whether the DOS near the band edge will follow any scaling law. The reasons are the following. It has been shown that, on the band edges of the pure coupled chains, the wavevector of the wavefunction depends on the magnetic field in a non-trivial way (Rammal *et al* 1983). When the coupled chains become random, it is not known how the reduction to the WNM can be made. It has also been shown that, when the magnetic field is above a critical value $\bar{\gamma}_1$, the amplitude of the localised states (if they appear) are always oscillatory (Jing and Zhang 1989). This makes the previously used theoretical methods, such as the variational approach of HL and the non-analytic weak-disorder expansion of Derrida and Gardner (1984), inapplicable. However, we can study this problem using the following approach. Since the analytic GF and its singularities near the band edges of the pure system are known, the scaling relations in region I can be obtained using the band CPA equation. If the scaling behaviour exists near the band edge, it is natural to extend the scaling relations found in region I to region II. The existence of the entire scaling region will finally be checked by the numerical simulation data.

In this work, we consider only the case of diagonal disorder. The site energies are random with a Gaussian distribution of various $W$. For any given $W$ and magnetic field $\gamma$, the DOS is simulated using the method of Dean (1972). It is found that the DOS near the band edges indeed follow a scaling function which is just the one-dimensional universal function when the magnetic field is above a critical value $\bar{\gamma}_1$. Below this critical field, a non-universal energy shift is required before the scaling can apply. The existence of such a non-universal shift limits the range of the scaling to a smaller $W$. In general, a magnetic-field-dependent effective one-dimensional band width can be defined near the band edge which also determines the scaling range of $W$. The scaling range of $W$ is strongly suppressed as the critical field $\bar{\gamma}_1$ is approached from both sides.

Before we examine the scaling behaviour near the band edge, we shall first discuss the overall feature of the DOS under various magnetic fields. Here two methods are used. Analytically, using the known GF of the pure system, CPA calculations can be carried out. Numerically, the DOS can also be obtained using Dean's method. On comparison with the simulation data, the CPA is shown to give very good results quantitatively except in the near-tail region (region II). In § 2, we shall briefly describe the model and outline the results of the analytic GFs obtained previously. The results of the CPA calculations will also be given. The scaling behaviour near the band edge will be discussed in detail in § 3 where the scaling relations are first obtained using the band CPA equation in region

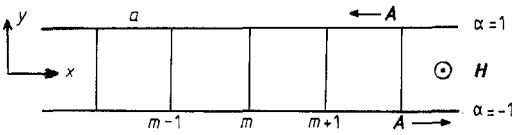


**Figure 1.** A tight-binding electron on coupled chains in a uniform magnetic field $\boldsymbol{H}$. $\boldsymbol{A}$ is the vector potential, $m$ is the position of a site along a chain with the lattice constant $a$ whereas $\alpha = +1$ and $\alpha = -1$ stand for the upper and lower chains, respectively.

I and then the existence of the entire scaling region is confirmed by the numerical simulations. The conclusions will be given in § 4.

## 2. The model and CPA calculations

Consider a single-band tight-binding electron on coupled chains as shown in figure 1. Let $\varepsilon_m$ be the site energy and $t$ be the constant-hopping matrix between the nearest-neighbour sites both in the same chain and in different chains. When a uniform magnetic field $\boldsymbol{H}$ is applied perpendicular to the ladder with $\boldsymbol{H} = H\hat{z}$ $(H > 0)$ and vector potential $\boldsymbol{A} = (-Hy, 0, 0)$, the corresponding Hamiltonian, in the Wannier representation, can be written as

$$H = \sum_{m,\alpha=\pm1} \varepsilon_m |m, \alpha\rangle\langle m, \alpha| + t \sum_{m,\alpha=\pm1} |m, \alpha\rangle\langle m, -\alpha| + t \sum_{m,\alpha=\pm1} \left[\exp\left(\frac{-i\gamma\alpha}{2}\right)|m+1, \alpha\rangle\langle m, \alpha| + \exp\left(\frac{i\gamma\alpha}{2}\right)|m, \alpha\rangle\langle m+1, \alpha|\right] \tag{1}$$

where $m$ is the position of a site along a chain ($x$ coordinate) whereas $\alpha = 1$ and $\alpha = -1$ stand for the upper and lower chains, respectively ($y$ coordinate) (figure 1). The value of $\gamma$ is determined by the magnetic field through the relation $\gamma = 2\pi\phi/\phi_0$ where $\phi_0$ $(= hc/e)$ is a flux quantum and $\phi$ $(= Ha^2)$ is the flux passing through a unit cell of lattice constant $a$. Here, for simplicity, we have assumed the same matrix $t$ for both intra-chain and inter-chain hoppings and a square unit cell. When $\varepsilon_m$ is a constant $\varepsilon_0$, the (diagonal) GF of the pure system has been evaluated by the present authors (Zhang and Jing 1989). Here we shall write down some useful results. Let $z = E \pm i\eta$ the GF has the following form:

$$G(z - \varepsilon_0, \gamma) = (1/2i\sqrt{x})\{[a_+ \cos(\gamma/2) - (z - \varepsilon_0)]/\sqrt{w_+} - [a_- \cos(\gamma/2) - (z - \varepsilon_0)]/\sqrt{w_-}\} \tag{2}$$

where

$$a_\pm(z - \varepsilon_0, \gamma) = (z - \varepsilon_0)\cos(\gamma/2) \pm i\sqrt{x} \tag{3}$$

$$w_\pm(z - \varepsilon_0, \gamma) = a_\pm^2 - 4t^2 \tag{4}$$

$$x(z-\varepsilon_0,\gamma)=[(z-\varepsilon_0)^2-f^2(\gamma)]\sin^2(\gamma/2) \tag{5}$$

and

$$f(\gamma)=t\sqrt{4+1/\sin^2(\gamma/2)}. \tag{6}$$

Since the functions $\sqrt{x}$ and $\sqrt{w_\pm}$ in equation (2) are multi-valued, certain branch cuts have to be drawn in order to determine their values. For the function $\sqrt{x}$, we have chosen a branch cut between the points $-f(\gamma)$ and $f(\gamma)$ on the real axis of the $z-\varepsilon_0$ plane, while for the function $\sqrt{w_+}$ (or $\sqrt{w_-}$) a branch cut between the points $-2t$ and $2t$ on the real axis of the $a_+$ (or $a_-$) plane has been drawn. Using the above procedure, the GF of equation (2) can be evaluated explicitly. It is not difficult to show that the symmetry relation $G(z-\varepsilon_0, 2\pi-\gamma)=G(z-\varepsilon_0,\gamma)$ exists and we only have to consider the magnetic field in the region $0\leqslant\gamma\leqslant\pi$. In our previous work, three different types of GF have been found in the following regions; $0\leqslant\gamma<\bar{\gamma}_1$, $\bar{\gamma}_1<\gamma<\bar{\gamma}_2$ and $\bar{\gamma}_2<\gamma\leqslant\pi$, where $\bar{\gamma}_1$ and $\bar{\gamma}_2$ are determined by the relations

$$\cos(\bar{\gamma}_1/2)=2\sin^2(\bar{\gamma}_1/2) \qquad \cos(\bar{\gamma}_2/2)=\tfrac{1}{2} \tag{7}$$

with the values $\bar{\gamma}_1\simeq 0.43\pi$ and $\bar{\gamma}_2=2\pi/3$.

When $\varepsilon_m$ is random with a Gaussian distribution $P(\varepsilon_m)$ of variance $W$, using equation (2), one can perform a CPA calculation in the presence of any magnetic field. The self-energy $\Sigma(E,\gamma)$ is determined from the usual CPA equation

$$\Sigma(E,\gamma)=\int \mathrm{d}\varepsilon_m\, P(\varepsilon_m)\frac{\varepsilon_m}{1-(\varepsilon_m-\Sigma)G(E-\Sigma)} \tag{8}$$

where $G(E-\Sigma)$ is given by equation (2) with $\varepsilon_0=\Sigma$. For any given complex number $\Sigma$, similar branch cuts can be drawn to evaluate $G(E-\Sigma)$ explicitly. The self-consistent solution of equation (8) gives the DOS, i.e. $\rho_{\mathrm{CPA}}(E)=-(1/\pi)\,\mathrm{Im}[G(E-\Sigma)]$. In figures 2(*a*), 2(*b*) and 2(c) the CPA results in the three different regions: $\gamma=0.40\,\pi$, $\gamma=0.62\,\pi$ and $\gamma=0.90\,\pi$, which are plotted (full curves) for the case $W/t=0.4$. In the numerical calculations, we have taken $t=1$, or equivalently, taken $t$ as the energy unit. These results are compared with the numerically simulated DOS histograms. Since the DOS is symmetric with respect to $E=0$, only the $E\geqslant 0$ half-space has been drawn. The CPA is able to give quantitatively good results for all three regions of $\gamma$ except in the near-tail region (region II as discussed in § 1) where the CPA always underestimates the DOS as expected. This is also true when $W/t=1$. In this case, the DOS becomes smoother and has less structure. In figure 2, we have also plotted the DOS of the pure system ($W/t=0$) (broken curves) for comparison.

## 3. Universal scaling near the band edge

As mentioned in § 1, the wavevector $\boldsymbol{k}$ of the wavefunction on the band edges of the pure system depends on the magnetic field $\gamma$ in the following non-trivial way (Rammal *et al* 1983); when $\gamma<\bar{\gamma}_1$, $k=0$, and, when $\gamma\geqslant\bar{\gamma}_1$,

$$2\cos k\sin^2(\gamma/2)=\cos(\gamma/2)\sqrt{1+4\sin^2 k\sin^2(\gamma/2)}.$$

Thus, it is not known how the reduction to the WNM can be made. Also because when $\gamma>\bar{\gamma}_1$, the amplitude of the localised states will always be oscillatory (Jing and Zhang 1989), it is not clear whether the entire scaling region of the DOS near the band edges

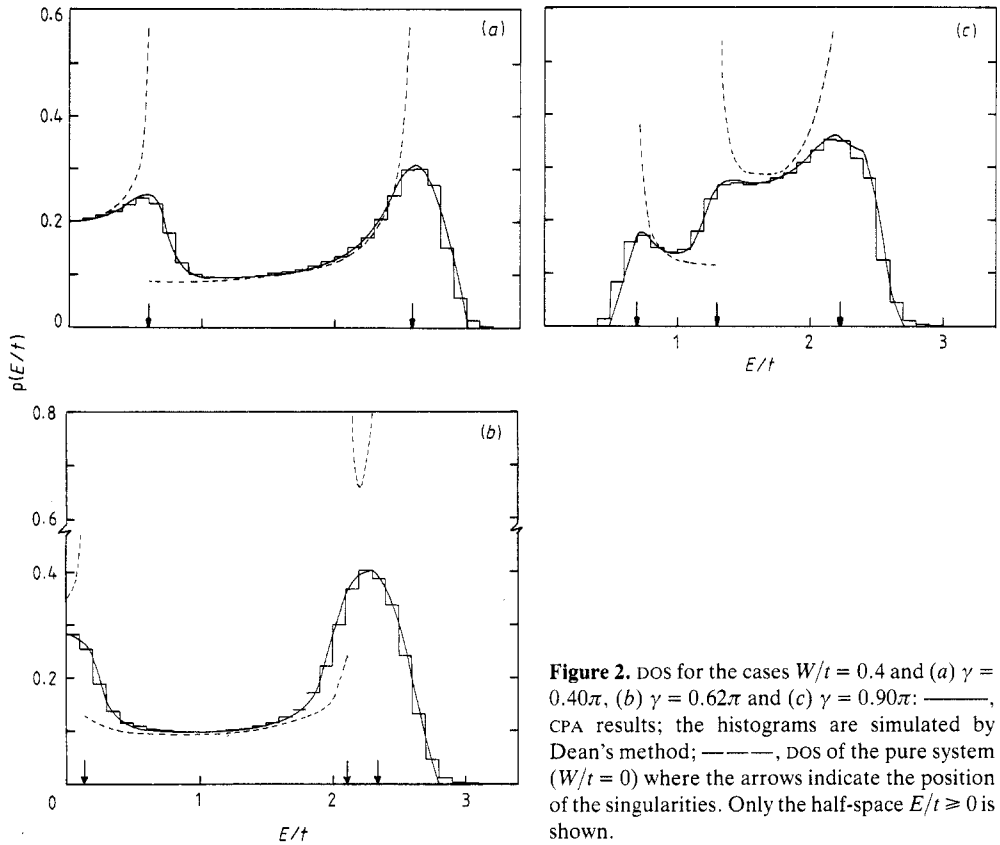


**Figure 2.** DOS for the cases $W/t = 0.4$ and (*a*) $\gamma = 0.40\pi$, (*b*) $\gamma = 0.62\pi$ and (*c*) $\gamma = 0.90\pi$: ———, CPA results; the histograms are simulated by Dean's method; — — —, DOS of the pure system ($W/t = 0$) where the arrows indicate the position of the singularities. Only the half-space $E/t \geq 0$ is shown.

found in the one-dimensional case will still be valid in the case of coupled chains under a magnetic field. To study this problem, as mentioned in § 1, we use the following procedure. Taking into account the fact that the singularities at the band edges are one dimensional, we use the effective-medium approach of Economou *et al* (1985) to derive a one-dimensional scaling relation for the self-energy with an effective one-dimensional band width. We simply assume that the natural length unit is also one dimensional. If scaling exists near the band edge, the scaling relations found in region I is expected to extend to region II and to form an entire scaling region near the band edge. The dimensionless DOS can then be obtained in terms of the dimensionless energy. The questions of the validity of our assumption and the existence of the scaling behaviour will finally be answered by the numerical data. Following Economou *et al* (1985), in the weak-disorder limit, equation (8) can be expanded as

$$\Sigma(E, \gamma) \simeq W^2 G(E - \Sigma) + O(W^4). \tag{9}$$

Near the upper band edge (UBE) of region I, the function $G(E - \Sigma)$ just outside the continuous spectrum can be obtained from equation (2). It can be shown from equation (2) that the singularities of the GF $G(E - \varepsilon_0)$ at the band edges are given by the factors $1/\sqrt{w_+}$ and $1/\sqrt{x}$ for $0 \leq \gamma < \bar{\gamma}_1$ and $\bar{\gamma}_1 < \gamma \leq \pi$, respectively. Thus, we consider these two cases separately.

*3.1.* $0 \leqslant \gamma < \bar{\gamma}_I$

In this case, the UBE is given by $w_+ = 0$ or $E_b = t[2\cos(\gamma/2) + 1]$. For energy slightly outside $E_b$, $E = E_b + \Delta E$, it can be shown from equation (2) that the GF has the following behaviour:

$$G(E - \Sigma) \simeq 1/\sqrt{4V(\Delta E - \Sigma)} + D(E, \gamma) \tag{10}$$

with

$$V(\gamma) = 4t[\cos(\gamma/2) - 2\sin^2(\gamma/2)], \tag{11}$$

and $D$ is a function of $\gamma$ and $E$. If $W$ is sufficiently small, we can approximate $D$ by its value at the UBE $E_b$ in which case $D$ has the following form:

$$D_b(\gamma) \equiv D(E_b, \gamma)$$

$$= \frac{[\cos\gamma - 2\sin\gamma\sin(\gamma/2)]}{4t[\cos(\gamma/2) - 2\sin^2(\gamma/2)]\sqrt{[cos\,\gamma + cos(\gamma/2)]^2 - 1}}. \tag{12}$$

Substituting equation (10) into equation (9), we have

$$\Sigma \simeq W^2/\sqrt{4V(\Delta E - \Sigma)} + W^2 D_b. \tag{13}$$

Equation (13) can be rewritten as

$$\bar{\Sigma}^3 - \bar{E}\bar{\Sigma}^2 + \tfrac{1}{4} = 0 \tag{14}$$

with

$$\bar{E} = (\Delta E - W^2 D_b)/\varepsilon_{01} \qquad \bar{\Sigma} = (\Sigma - W^2 D_b)/\varepsilon_{01} \tag{15}$$

and

$$\varepsilon_{01} = (W^4/V)^{1/3}. \tag{16}$$

Equations (14) and (16) are the typical one-dimensional results with $4V$ as the effective band-width. Here, the energy $\Delta E$ should be shifted by a non-universal value $W^2 D_b$ before scaling can apply. However, unlike the WNM in dimensions $2 \leqslant d < 4$, this non-universal energy shift is not caused by the existence of a lattice constant to remove the ultraviolet divergence. Since the energy unit $\varepsilon_{01}$ is one dimensional, we shall also take the one-dimensional length unit $L_{01} = W^{-2/3}V^{2/3}a$ as the natural length (Economou *et al* 1985). Thus, if the entire scaling region exists near the band edge, the dimensionless DOS $\bar{\rho}(\bar{E}) = \rho(E)L_{01}\varepsilon_{01}$ as a function of the shifted and scaled energy $\bar{E}$ should be a universal function in both region I and region II. It is plausible to guess that this universal function is identical with the one-dimensional universal function which has the form (Derrida and Gardner 1984)

$$\bar{\rho}(\bar{E}) = \sqrt{2/\pi}\, N_+/N_-^2 \tag{17}$$

with

$$N_\pm = \int_0^\infty \mathrm{d}t/t^{\pm 1/2} \exp(-\tfrac{1}{6}t^3 + 2\bar{E}t). \tag{18}$$

Numerically, the DOS is simulated using Dean's method for coupled chains of length $10^4$ lattice constants and the results of 15–20 configurations are averaged depending on

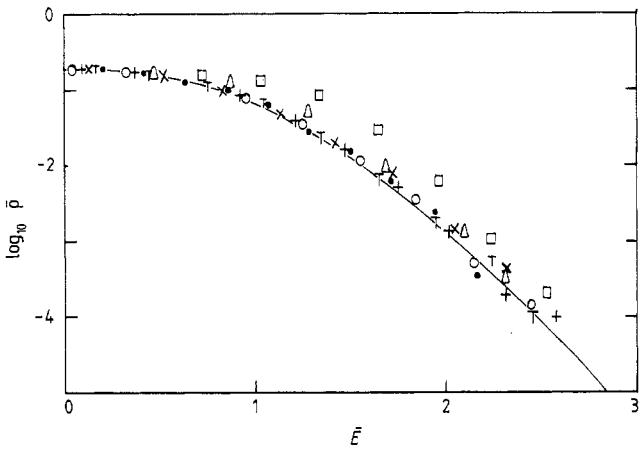


**Figure 3.** For $0 \leq \gamma < \bar{\gamma}_1 \simeq 0.43\pi$, a plot of the dimensionless DOS as a function of the shifted and scaled energy $\bar{E}$: ———, result of equation (17); ●, $W/t = 0.4$, $\gamma = 0.00$; ×, $W/t = 0.4$, $\gamma = 0.08\pi$; ○, $W/t = 0.4$, $\gamma = 0.16\pi$; +, $W/t = 0.4$, $\gamma = 0.24\pi$; T, $W/t = 0.4$, $\gamma = 0.28\pi$; △, $W/t = 0.4$, $\gamma = 0.36\pi$; □, $W/t = 0.4$, $\gamma = 0.38\pi$.

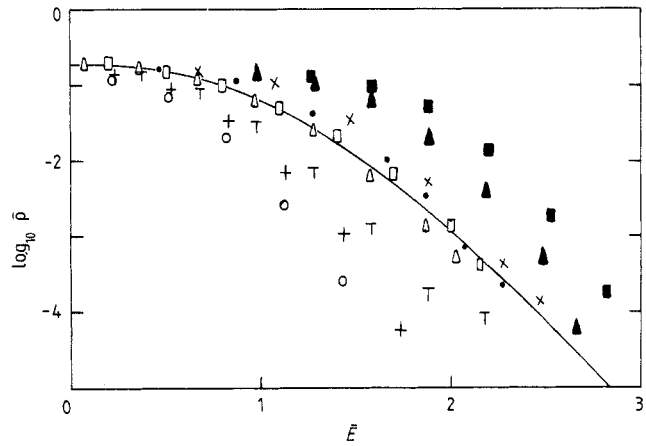


**Figure 4.** For $\gamma \simeq \bar{\gamma}_1$, a plot of the dimensionless DOS as a function of the scaled energy $\bar{E}$ (also shifted when $\gamma < \bar{\gamma}_1$): ———, result of equation (17); □, $W/t = 0.01$, $\gamma = 0.40\pi$; ●, $W/t = 0.05$, $\gamma = 0.40\pi$; ×, $W/t = 0.10$, $\gamma = 0.40\pi$; ▲, $W/t = 0.20$, $\gamma = 0.40\pi$; ■, $W/t = 0.30$, $\gamma = 0.40\pi$; △, $W/t = 0.01$, $\gamma = 0.46\pi$; T, $W/t = 0.05$, $\gamma = 0.46\pi$; +, $W/t = 0.10$, $\gamma = 0.46\pi$; ○, $W/t = 0.20$, $\gamma = 0.46\pi$.

the value of $W$ and $\gamma$. In figure 3 the function $\log_{10}\bar{\rho}(\bar{E})$ is plotted against the shifted and scaled energy $\bar{E}$ of equation (15) for $W/t = 0.4$ and various values of $\gamma$. The full curve is the result of equation (17). Except for the cases $\gamma = 0.36\pi$ and $0.38\pi$, the scaling of $\gamma$ does exist and follows the one-dimensional universal function of equation (17). There is a systematic deviation from equation (17) as $\gamma$ approaches $\bar{\gamma}_1$ ($\simeq 0.43\pi$). This is because, when $\bar{\gamma}_1$ is approached, the effective band width $4V$ of equation (11) shrinks to zero as can be seen from equation (7) and the scaling range of $W$ is strongly suppressed. Thus, we would expect that, even when $\gamma$ is very close to $\bar{\gamma}_1$, scaling will exist when $W$ is sufficiently small. This is shown in figure 4 when $\gamma = 0.40\pi$. The function $\log_{10}\bar{\rho}(\bar{E})$

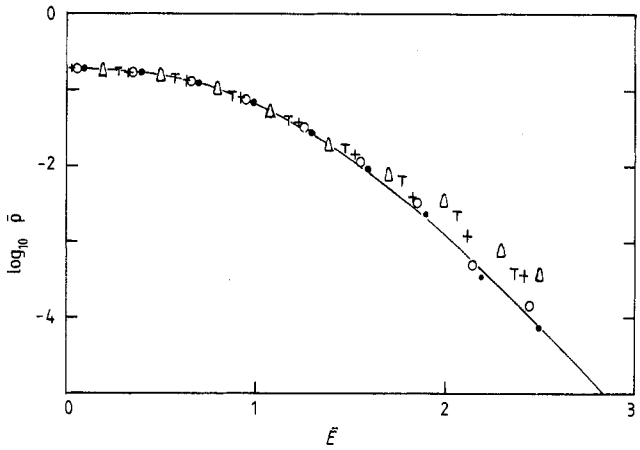


**Figure 5.** For $0 \leqslant \gamma < \bar{\gamma}_1 \simeq 0.43\pi$, a plot of the dimensionless DOS as a function of the shifted and scaled energy $\bar{E}$: ——, result of equation (17); ●, $W/t = 0.2$, $\gamma = 0.16\pi$; ○, $W/t = 0.4, \gamma = 0.16\pi$; +, $W/t = 0.6, \gamma = 0.16\pi$; △, $W/t = 0.8, \gamma = 0.16\pi$; T, $W/t = 1.0, \gamma = 0.16\pi$.

indeed approaches the result of equation (17) as $W/t$ becomes smaller than 0.01. For a fixed $\gamma = 0.16\pi$, we have also plotted the function $\log_{10}\bar{\rho}(\bar{E})$ for various values of $W/t$ in figure 5. The systematic deviation from the scaling function as $W/t$ is increased above 0.4 is due to the invalidity of the constant energy shift $D_b$ given in equation (12). Thus the existence of this energy shift also suppresses the range of scaling.

If we roughly define region I as the region where the DOS is higher than one fifth of its maximum value near the band edge (see figure 2 for instance), then regions I and II are roughly separated by $\bar{E} \simeq 1.2$ which is consistent with the value found in figure 4 of Economou *et al* (1985). Figures 3–5 do confirm that the entire scaling region exists and follows the one-dimensional universal function. The accuracy of our numerical data is limited by the finite number of configurations used. As $\bar{E}$ is farther away from the band edge, the smoothness of the DOS gives large fluctuations in the numerical data and more configurations are required to give a reliable result. The error bars for figures 3–5 vary from less than the size of the symbols for $\bar{E} \leqslant 1$ to about twice the size of symbols for $\bar{E} \geqslant 2$.

### 3.2. $\bar{\gamma}_1 < \gamma \leqslant \pi$

In this case, the UBE is given by the condition $x = 0$ or $E_b = f(\gamma)$ of equation (6). For energies slightly outside $E_b$, $E = E_b + \Delta E$, it can be shown from equation (2) that the GF behaves like

$$G(E - \Sigma) \simeq 1/\sqrt{4V(\Delta E - \Sigma)} \tag{19}$$

with

$$V = t^2[\cos^2(\gamma/2) - 4\sin^4(\gamma/2)]/2f(\gamma)\sin^4(\gamma/2) \tag{20}$$

where $f(\gamma)$ is given by equation (6). When equation (19) is compared with equation (10), it is easy to see that scaling (if it exists) will again be one-dimensional with $\varepsilon_{01}$ and $L_{01}$ as the energy and length units, except now $V$ is given by equation (20). In this case, no energy shift is required before scaling can apply. Thus, unlike the case in § 3.1, here, the

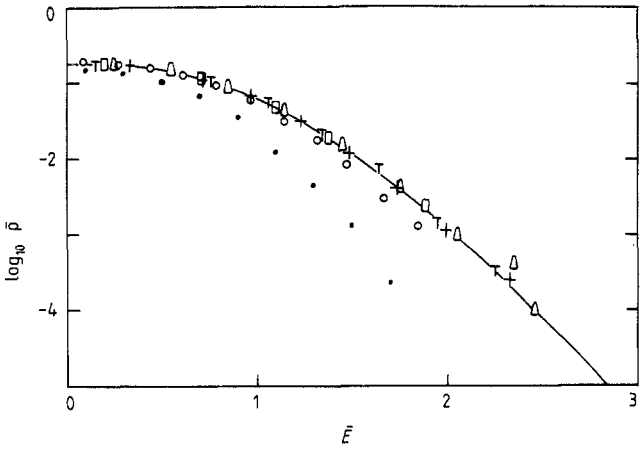


**Figure 6.** For $\pi \geqslant \gamma > \bar{\gamma}_1 \simeq 0.43\pi$, a plot of the dimensionless DOS as a function of the scaled energy $\bar{E}$: ———, result of equation (17); ●, $W/t = 0.4$, $\gamma = 0.5\pi$; ○, $W/t = 0.4$, $\gamma = 0.6\pi$; T, $W/t = 0.4$, $\gamma = 0.7\pi$; +, $W/t = 0.4$, $\gamma = 0.8\pi$; □, $W/t = 0.4$, $\gamma = 0.9\pi$; △, $W/t = 0.4$, $\gamma = \pi$.

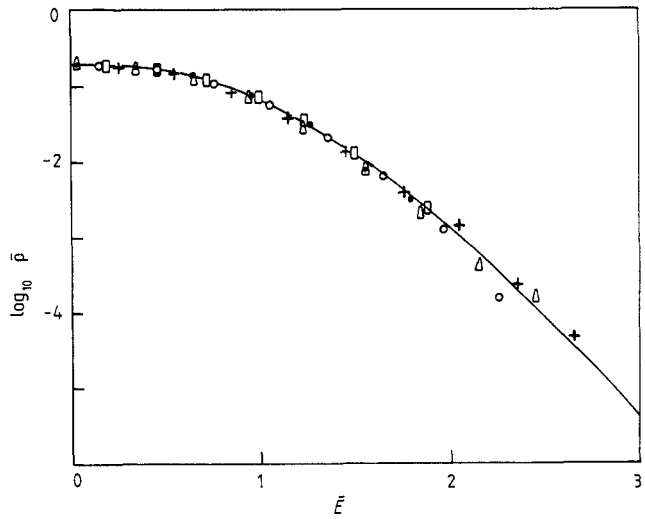


**Figure 7.** For $\pi \geqslant \gamma > \bar{\gamma}_1 \simeq 0.43\pi$, a plot of the dimensionless DOS as a function of scaled energy $\bar{E}$: ———, result of equation (17); ○, $W/t = 0.2$, $\gamma = 0.9\pi$; □, $W/t = 0.4$, $\gamma = 0.9\pi$; ●, $W/t = 0.6$, $\gamma = 0.9\pi$; △ = $W/t = 0.8$, $\gamma = 0.9\pi$; +, $W/t = 1.0$, $\gamma = 0.9\pi$.

scaling range of $W/t$ is limited by the effective band width $4V$ of equation (20) alone. In figure 6 the function $\log_{10}\bar{\rho}(\bar{E})$ is plotted for $W/t = 0.4$ and various values of $\gamma$. For $\gamma$ in the region $0.6\pi < \gamma \leqslant \pi$, the scaling holds pretty well and follows the one-dimensional universal function. As $\gamma < 0.6\pi$, the systematic deviation is due to the shrinking of the effective band width $4V$ of equation (20) when $\bar{\gamma}_1$ is approached. This shrinking again limits the scaling to a smaller value of $W/t$. This is demonstrated in figure 4 with $\gamma = 0.46\pi$. There is a systematic approach to the universal function in equation (17) as $W/t$ is decreased and the scaling seems to hold when $W/t < 0.01$. Finally, in figure 7, we have

plotted the function $\log_{10}\bar{\rho}(\bar{E})$ for the fixed value of $\gamma = 0.9\pi$ and different values of $W/t$. Unlike the case in § 3.1 (as shown in figure 5), here, the scaling holds even when $W/t = 1.0$ owing to the absence of the energy shift $D_b$.

## 4. Conclusions

In this work, we have studied the DOS and its scaling behaviour near the band edges of weakly disordered coupled chains in a magnetic field. Only the site energies are considered to be random with a Gaussian distribution of variance $W$. On comparison with the simulation data obtained using Dean's method, except in the near-tail regions the CPA is shown to give quantitatively good results for all three different kinds of GF in various magnetic fields (figure 2). The scaling behaviour in the near-band-edge regions has been studied in detail. The scaling relations found from the band CPA equation in region I is naturally extended to the near-tail region (region II) and the existence of the entire scaling region near the band edge is confirmed numerically. Moreover, an effective one-dimensional band width can be defined and the scaling law is such that the DOS follows the usual one-dimensional universal function. This effective band width shrinks to zero as the critical field $\bar{\gamma}_1$ ($\simeq 0.43\pi$) is approached from both sides. This shrinking strongly suppresses the scaling range of $W/t$. Below the critical field $\bar{\gamma}_1$, a non-universal energy shift is required before the scaling can apply. The existence of this energy shift also limits the range of scaling to a smaller $W/t$.

## Acknowledgments

The authors would like to thank the referee for useful comments on the original manuscript. The work was supported by the National Science Foundation of China.

## References

Cohen M H, Economou E N and Soukoulis C M 1985 *Phys. Rev.* B **32** 8268
Dean P 1972 *Rev. Mod. Phys.* **44** 127
Derrida B and Gardner E 1984 *J. Physique* **45** 1283
Economou E N, Soukoulis C M, Cohen M H and Zdetsis A D 1985 *Phys. Rev.* B **31** 6172
Evangelou S N 1987 *J. Phys. C: Solid State Phys.* **20** L89
Halperin B I 1965 *Phys. Rev.* **139** A 104
Halperin B I and Lax M 1966 *Phys. Rev.* **148** 722
Jing X D and Zhang Z Q 1989 *Phys. Rev.* B **39** 11434
Rammal R, Lubensky T C and Toulouse G 1983 *Phys. Rev.* B **27** 2820
Zhang Z Q and Jing X D 1989 *Phys. Rev.* B **39** 11428
Zhang Z Q and Sheng P 1986 *Phys. Rev. Lett.* **57** 909